Comparison of Source Images for Protons, π^-'s, and Λ's in 6A GeV Au + Au Collisions

P. Chung,[1] N. N. Ajitanand,[1] J. M. Alexander,[1] M. Anderson,[4] D. Best,[5] F. P. Brady,[4] T. Case,[5] W. Caskey,[4] D. Cebra,[4] J. L. Chance,[4] B. Cole,[9] K. Crowe,[5] A. C. Das,[2] J. E. Draper,[4] M. L. Gilkes,[1] S. Gushue,[1,7] M. Heffner,[4,13] A. S. Hirsch,[12] E. L. Hjort,[12] W. Holzmann,[1] L. Huo,[11] M. Issah,[1] M. Justice,[3] M. Kaplan,[6] D. Keane,[3] J. C. Kintner,[10] J. Klay,[4] D. Krofcheck,[8] R. A. Lacey,[1] J. Lauret,[1] M. A. Lisa,[2] H. Liu,[3] Y. M. Liu,[11] R. McGrath,[1] Z. Milosevich,[6] G. Odyniec,[5] D. L. Olson,[5] S. Panitkin,[3] N. T. Porile,[12] G. Rai,[5] H. G. Ritter,[5] J. L. Romero,[4] R. Scharenberg,[12] B. Srivastava,[12] N. T. B Stone,[5] T. J. M. Symons,[5] A. Taranenko,[1] J. Whitfield,[6] R. Witt,[3] L. Wood,[4] and W. N. Zhang[11]

(E895 Collaboration)

[1]*Departments of Chemistry and Physics, SUNY, Stony Brook, New York 11794-3400, USA*
[2]*Ohio State University, Columbus, Ohio 43210, USA*
[3]*Kent State University, Kent, Ohio 44242, USA*
[4]*University of California, Davis, California 95616, USA*
[5]*Lawrence Berkeley National Laboratory, Berkeley, California 94720, USA*
[6]*Carnegie Mellon University, Pittsburgh, Pennsylvania 15213, USA*
[7]*Brookhaven National Laboratory, Upton, New York 11973, USA*
[8]*University of Auckland, Auckland, New Zealand*
[9]*Columbia University, New York, New York 10027, USA*
[10]*St. Mary's College, Moraga, California 94575, USA*
[11]*Harbin Institute of Technology, Harbin, 150001 People's Republic of China*
[12]*Purdue University, West Lafayette, Indiana 47907-1396, USA*

D. Brown,[13] S. Pratt,[14] F. Wang,[15] and P. Danielewicz[14]

[13]*Livermore National Laboratory, Livermore, California 94550, USA*
[14]*National Superconducting Cyclotron Laboratory, Michigan State University, East Lansing, Michigan 48824, USA*
[15]*Purdue University, West Lafayette, Indiana 47907-1396, USA*

(Received 28 December 2002; published 14 October 2003)

Source images are extracted from two-particle correlations constructed from strange and nonstrange hadrons produced in 6A GeV Au + Au collisions. Very different source images result from pp vs $p\Lambda$ vs $\pi^-\pi^-$ correlations. Scaling by transverse mass can describe the apparent source size ratio for p/π^- but not for Λ/π^- or Λ/p. These observations suggest important differences in the space-time emission histories for protons, pions, and neutral strange baryons produced in the same events.

DOI: 10.1103/PhysRevLett.91.162301 PACS numbers: 25.75.Ld

Relativistic heavy ion collisions of (1–10)A GeV produce a fireball of nuclear matter with extremely high baryon and energy density [1]. The dynamical evolution of this fireball is driven by such fundamental properties as the nuclear equation of state and possibly by a phase transition, e.g., to a quark gluon plasma [2–6]. Two-particle correlation studies, for various particle species, provide an important probe of the space-time extent of this fireball [7–10]. Recent model calculations suggest that the time scale for freeze-out of strange and multi-strange particles may be much shorter than that for non-strange particles [11,12], implying a much smaller space-time emission zone for strange particles. If this is indeed the case, then correlation studies involving strange particles may serve as important "signposts" for dynamical backtracking into the very early stage of the collision where large energy densities are achieved [13].

In this Letter, we compare the source properties for protons, π^-'s, and Λ hyperons extracted from pp, $\pi^-\pi^-$, and $p\Lambda$ correlation functions, as produced in 6A GeV Au + Au collisions. These data are unique in that they constitute the first measurement of $p\Lambda$ correlations. If Λ hyperons are in fact emitted from a source with a smaller space-time extent, then, between this and π^- source broadening from resonance decays, one might naively expect an ordering of two-particle source sizes: $R_{p\Lambda} < R_{pp} < R_{\pi\pi}$. On the other hand, it is known that at these energies the three-dimensional π^- radii exhibits m_T scaling [7,14] and this should manifest itself in the angle-averaged π^- sources. Furthermore, since m_T scaling can be ascribed to position-momentum correlations in the particle emission function [15], one might expect similar effects in the pp and $p\Lambda$ sources. As we will show, neither an interpretation based solely on

position-momentum correlations nor on naive geometrical arguments can fully account for the relative size of the three sources.

Traditional correlation analyses rely on the weakness of final-state interactions (FSI). With this, one may correct for FSI leaving a correlation that is the Fourier transform of the two-particle source function. This approximation is mostly valid for pions; for massive and/or strongly interacting particles, such as protons or Λ hyperons, this approximation breaks down. Recently, Brown and Danielewicz have presented an imaging technique for analyzing two-particle correlations [16]. The technique actually *uses* the FSI, encoded in the form of the particles' final-state wave function, to extract the two-particle source function *directly* [16]. The imaging technique has been used to address only a few data sets. Panitkin *et al.* [17] have shown that this approach gives source radii similar to the conventional Hanbery, Brown, and Twist (HBT) approach (under the assumption of a Gaussian source) for $\pi^-\pi^-$ pairs emitted in central collisions for (2–8)A GeV Au + Au. By contrast, Verde *et al.* [18] have shown very different results for pp pairs from 75A MeV ^{14}N + ^{197}Au. For our purpose, the imaging technique's key feature is that one can easily compare source functions across different species and assess the different space-time scales relevant for each particle pair — a feature that has been mentioned [16], but never seriously utilized.

We use the imaging technique on pp, $\pi^-\pi^-$, and $p\Lambda$ pairs to extract and compare the source properties for protons, π^-'s, and Λ hyperons. The measurements have been performed with the E895 detector at the Brookhaven Alternating Gradient Synchrotron. Here, we concentrate on the construction of the $p\Lambda$ and pp correlations and the results of the imaging analysis. Details on the detector and its setup have been reported elsewhere [6,19,20].

We reconstructed the Λ's from the daughters of their charged particle decay, $\Lambda \rightarrow p + \pi^-$ (branching ratio $\simeq 64\%$), following the procedure outlined in Ref. [19]. Figure 1 shows the invariant mass spectrum for Λ's obtained in semicentral (upper 23% of total inelastic cross section, $b \lesssim 7$ fm) 6A GeV Au + Au collisions. For the $p\Lambda$ correlation analysis, an enriched sample ($\sim 80\%$) of Λ's with $1.11 \leq M_\Lambda \leq 1.122$ GeV was used.

Figures 2(a)–2(c) show the correlation functions, $C(q)$, obtained by taking the ratio of foreground to background distributions in relative momentum for Λp, pp, and $\pi^-\pi^-$ pairs, respectively. Here, $q = \frac{1}{2}\sqrt{-(p_1 - p_2)^2}$ is half of the relative momentum between the two particles in the pair c.m. frame. We applied no explicit gates on transverse momentum and rapidity except those implicit in the tracking acceptance. The mean transverse momenta $\langle P_t \rangle$ for particles from pairs with $q < 50$ MeV were 0.3 and 0.12 GeV/c for pp and $\pi^-\pi^-$ pairs and the mean rapidities $\langle y \rangle$ were -0.33 and 0.1. The Λp pairs with $q < 50$ MeV have $\langle P_t \rangle = 0.46$ GeV/c and $\langle y \rangle = -0.18$ for Λ's and $\langle P_t \rangle = 0.38$ GeV/c and $\langle y \rangle = -0.18$ for protons.

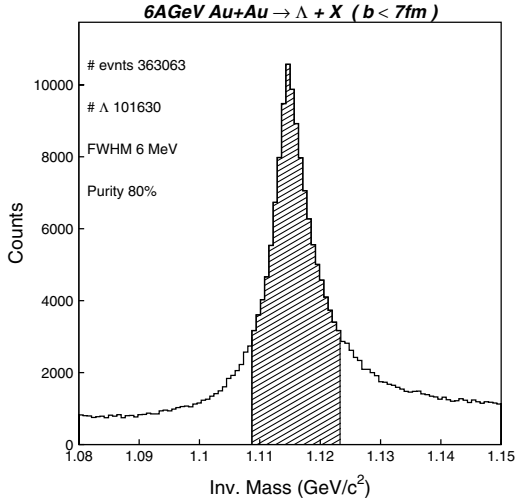

FIG. 1. Λ invariant mass spectrum from semicentral 6A GeV Au + Au collisions. The hatched area depicts the Λ mass gate used to select the Λ's for Λp correlation analysis.

We constructed the numerator (or foreground) distribution from pairs of particles from the same event, and obtained the denominator (or background) distribution by pairing particles from different events. We used a track-merging filter similar to that outlined in Ref. [7] to eliminate possible distortions resulting from track-merging effects in the time projection chamber. For each correlation function, we used the accepted range of particle multiplicities to specify impact parameters

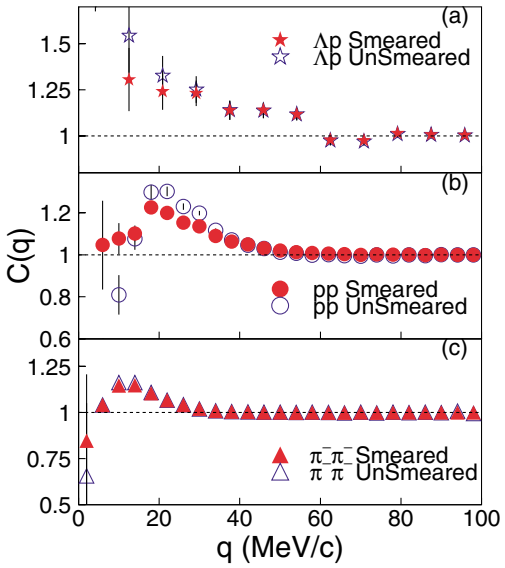

FIG. 2 (color online). Raw smeared (filled symbols) and corrected unsmeared (open symbols) correlation functions, $C(q)$, for (a) Λp, (b) pp, and (c) $\pi^-\pi^-$ from 6A GeV Au + Au collisions ($b < 7$ fm).

$b < 7$ fm. This range was chosen to optimize the statistical significance for $p\Lambda$ pairs.

We utilized approximately 100 000 Λ's (80% purity) to yield about 31 000 Λp pairs in the foreground distribution, with $q \leq 100$ MeV/c, after applying the track-merging cut for the 6A GeV data. We have corrected the Λp correlation function for (i) the combinatoric background ($\simeq$20%) included in the Λ sample, (ii) the feed down due to the electromagnetic decay of the Σ^0 (estimated to be $\simeq 25\%$ from relativistic quantum molecular dynamics calculations), and (iii) the smearing due to the momentum resolution of the detector.

We corrected the sources for the momentum resolution using two independent methods, both leading to consistent results. In the first method, we left the data uncorrected and modified the kernel used in the imaging analysis to include the smearing effect, assuming an average δp for each $\langle p_T \rangle$ and $\langle y \rangle$. This technique will be detailed elsewhere [21]. In the second method, we first corrected the correlation functions via an iterative procedure and imaged with an unsmeared kernel. We explain this procedure in the next paragraph. We determined the momentum resolution for π^- and p from GEANT simulations giving an average value of 2.0% and 3.1% for each component of the π^- and proton momentum resolution, respectively. For the Λ momentum resolution, we extracted an average value of 4.0% for each component of the resolution using the width of the Ξ^- mass peak (Ξ^- decays to $\Lambda\pi^-$) and the π^- momentum resolution.

Our iterative procedure starts with model calculations (Gaussian sources) for the particle momenta and their (unsmeared) correlations, $C_u(q)$. We then use a Monte Carlo method to smear their momenta and use these to calculate the smeared correlation $C_s(q)$. The ratio $C_s(q)/C_u(q)$ is used to make a first-try correction to the raw observed data correlation $C(q)$. This gives a first iteration unsmeared correlation $C'_u(q)$. The latter is then smeared in the second iteration (using pairs of particle from mixed data events) to give a second smeared correlation, $C'_s(q)$. Typically, the comparison between the raw observed $C(q)$ in the data and the second smeared correlation function led to a reduced $\chi^2 \simeq 1$. The associated function $C'_u(q)$ was then taken as the unsmeared correlation for the data. Figure 2 shows both smeared and unsmeared correlation functions. The results presented in this paper are from the iterative method.

The $p\Lambda$ correlations can lead to residual correlations between primary protons and daughter protons from Λ decays. Wang has calculated the magnitude of this residual effect on the pp correlation [22]. We have determined its effect on our pp correlations to be negligible. This is due to (i) the intrinsically small residual pp correlation (maximum 3%) arising from our observed $p\Lambda$ correlation and (ii) the small fraction of secondary protons resulting from Λ decay ($\approx$6% of the total number of protons). The same reasoning applies for the expected perturbation of $p\Lambda$ correlations from $\Lambda\Lambda$ correlations [23] and of $\pi^-\pi^-$ correlations from $\pi^-\Lambda$ or $\pi^- K^0$ correlations [24].

Figures 3(a)–3(c) show correlation functions for Λp, pp, and $\pi^-\pi^-$ pairs, respectively. We have not corrected the pp and $\pi^-\pi^-$ correlation functions for the Coulomb interaction since this effect is included in the imaging procedure. The two-particle correlation and the source function are related through the Koonin-Pratt equation [25]:

$$C(q) - 1 = 4\pi \int dr\, r^2 K(q, r) S(r). \qquad (1)$$

This is a linear integral equation that we may invert to obtain the source function $S(r)$ using the techniques in Ref. [16]. Here, the imaged source function $S(r)$ gives the probability of emitting a pair of particles a distance r apart in the pair c.m. frame. The derived source functions are shown in Figs. 3(d)–3(f). As a consistency check, we have recalculated the correlation functions from the derived source functions and these are shown in Figs. 3(a)–3(c) as restored correlations.

In Eq. (1), the kernel $K(q, r)$ encodes the FSI and is given in terms of the final-state wave function as $K(q, r) = \frac{1}{2}\int d(\cos(\theta_{\mathbf{q},\mathbf{r}}))[|\Phi_{\mathbf{q}}(\mathbf{r})|^2 - 1]$. In this work, we used the Coulomb force for the pion and proton pairs. Additionally, we used the Reid93 nucleon-nucleon force for protons [26] and the phenomenological potential of Bodmer and Usmani for Λp pairs [27]. Since the Λp potential is not very well known, we reanalyzed the $p\Lambda$ correlation using a simplified kernel that depends only on the $p\Lambda$ effective range and scattering length. We found no significant change in the imaged Λp source.

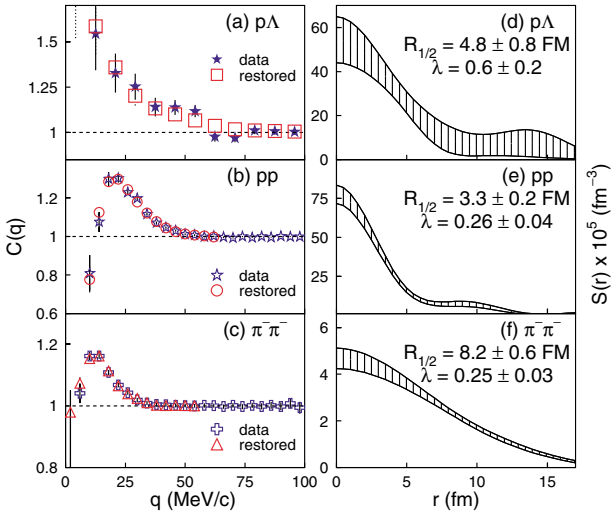

FIG. 3 (color online). Correlation functions, $C(q)$, for $p\Lambda$, pp, and $\pi^-\pi^-$ pairs are shown in panels (a), (b), and (c), respectively. The corresponding short-range source functions, $S(r)$, are indicated in panels (d), (e), and (f). As a consistency test, a simulated correlation function (open squares, circles, and triangles) is recalculated from $S(r)$. Hatched bands show the zone of one standard deviation.

The sources in Figs. 3(d)–3(f) appear Gaussian, although we cannot definitively conclude this given the size of the error bands on the imaged sources. In principle, the source function can be composed of an admixture of short- and large-range emission sources [16]. In practice, the shape of the correlation is strongly dominated by the short-range source, and the less-correlated pairs from any large-range source essentially dilute the strength of the observed correlation. Let us then assume a Gaussian for the short-distance part of the time integrated emission function for particle type i: $D_i \sim f_i \exp(-r^2/2R_i^2)$. The fraction of particles emitted from this source is $0 \leq f_i \leq 1$. This choice gives us a Gaussian two-particle source function for particles i and j:

$$S_{ij}(r) \propto \lambda_{ij} \exp[-r^2/2(R_i^2 + R_j^2)]. \quad (2)$$

To ensure that we use the same source parametrization for like and unlike pairs, we choose $R_{ij}^2 = \frac{1}{2}(R_i^2 + R_j^2)$. With this choice, the emission function radius is exactly the two-particle source radius if $i = j$ (i.e., $R_{ii} = R_i$) [28]. Here the fraction of pairs λ_{ij} is related to the fraction of particles in each emission function through $\lambda_{ij} = f_i f_j$. In all subsequent discussions, we take the $R_{1/2}$ value (the radius at half maximum density) directly from the sources, but we convert the source height into an equivalent Gaussian λ. Values for λ and $R_{1/2}$ of the short-range sources are indicated in Figs. 3(d)–3(f).

Figure 4 shows that there is relatively little dependence of $R_{1/2}$ on $\langle P_t \rangle$ over the measured range; the λ values for π^--π^-, on the other hand, do exhibit some change with $\langle P_t \rangle$ in contrast to the behavior for pp. Scanning Figs. 3(d)–3(f), the pion source is clearly the broadest. However, our naive expectation that the Λp source would be the smallest source appears wrong. In an effort to understand why, we investigate the source sizes in more detail.

Consider first the results in Figs. 3(c) and 3(f) for $\pi^-\pi^-$, where $R_{1/2} = 8.2 \pm 0.6$ fm. This radius, corresponding to a centrality range of $b < 7$ fm, is identical to that reported by Panitkin *et al.* for $b < 5$ fm [17,29]. The λ value of 0.25 ± 0.03 indicates that half of the pions arise from a source with $R_{1/2} \sim 8.2$ fm and the other half from a considerably larger source, possibly caused by resonance decays. For $p\Lambda$ pairs [cf. Figures 3(a) and 3(d)], the correlations are dominated by a source of intermediate size ($R_{1/2} = 4.8 \pm 0.8$ fm) comprising $60\% \pm 20\%$ of the $p\Lambda$ pairs.

The contrast between the $\pi^-\pi^-$ and pp sources is pronounced [cf. Figs. 3(b) and 3(e)]. The pp correlations are dominated by a very compact source $R_{1/2} = 3.3 \pm 0.2$ fm and this source comprises only 26% of the pairs or 51% of the total protons. Both in 75A MeV ^{14}N + ^{197}Au [18] and 200A GeV S + Pb [16] investigators have found relatively small source sizes ($R_{1/2} = 2.9$ fm and $R_{1/2} = 3.2$ fm, respectively) for roughly the same fraction of protons. From these observations, we suspect that there is a common feature in nucleus-nucleus collisions that span a broad range because (i) strong collective motion focuses the source to much smaller radii [30], and (ii) pp correlations are insensitive to the long distance parts of the source, as discussed by Wang and Pratt [13]. While we cannot separate these two effects in this study (or even rule out other more exotic causes), we comment that pions are much less focused by collective effects because of their much lower mass [31]. Consequently, we expect the pion correlation function to probe a larger portion of the emission region and, hence, be associated with a larger source.

Previous literature [7,14] indicated that the three-dimensional pion radii exhibit m_T scaling. $R_{1/2}$ in the pair c.m. frame can be computed from the three-dimensional source radii $R_{\rm out}$, $R_{\rm side}$, and $R_{\rm long}$ in the longitudinally comoving source (LCMS) frame via

$$R_{1/2} \approx 1.66\sqrt[3]{\gamma R_{\rm out} R_{\rm side} R_{\rm long}}, \quad (3)$$

where the Lorentz factor is $\gamma = m_T/m$. In the various models of m_T scaling of correlation radii, the radii in the LCMS frame all have the same form: $R = R^0\sqrt{T/m_T}$. Here T is the source temperature and the R^0's for each radius depend on the details of the model in question. Inserting this dependence into Eq. (3) gives

$$R_{1/2} \approx R_{1/2}^0 \sqrt{T/m_T^{\rm eff}}, \quad (4)$$

where $m_T^{\rm eff} = \sqrt[3]{m_T m^2}$. This implies that $R_{1/2}$ scales weakly as $m_T^{-1/6}$ regardless of the m_T scaling model.

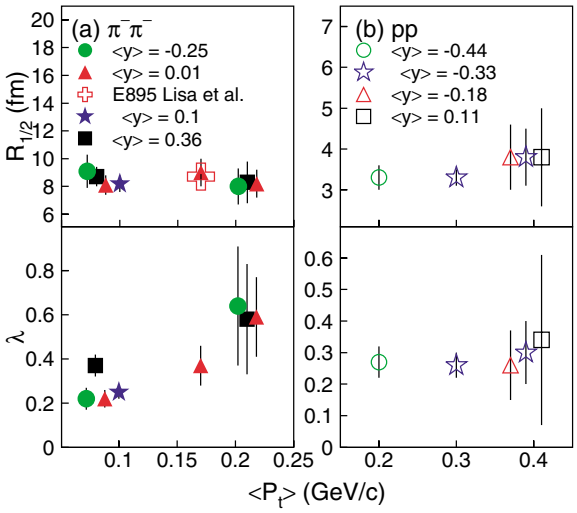

FIG. 4 (color online). Variation of source half-radius $R_{1/2}$ (top panels) and λ parameter (bottom panels) for different phase space regions identified by their mean transverse momentum $\langle P_t \rangle$ and mean rapidity $\langle y \rangle$ values (shown in different symbols) for sources from (a) $\pi^-\pi^-$ and (b) pp correlations. The open cross in (a) shows the $R_{1/2}$ value, calculated from the HBT radii from Ref. [7].

Using the $\langle P_t \rangle$'s indicated for the pion and proton pairs, we find that m_T scaling predicts the ratio $R_{pp}/R_{\pi^-\pi^-} = \sqrt{m^{\rm eff}_{T\pi^-}/m^{\rm eff}_{Tp}} = 0.4$, which is consistent with the value observed for the same experimental ratio (0.40 ± 0.04). In contrast to the pp and $\pi^-\pi^-$ sources, the $p\Lambda$ source size does not show an apparent m_T scaling. Naively applying Eq. (4) and keeping a constant temperature and geometrical source size, one obtains a predicted $p\Lambda$ source size of 3.1 ± 0.2 fm which is significantly smaller than the experimental value. This value cannot be accounted for via the proton-Λ mass difference of $\approx 20\%$ and could possibly reflect differences between the emission time and the collective focusing for Λ's and protons. The magnitude of collective flow for Λ's is known to be smaller than that for protons [32].

As a possibility, let us assume that the underlying proton emission function is common to both the pp and $p\Lambda$ correlations. For this assumption to hold, we must assume that any flow induced focusing affects the pp and $p\Lambda$ sources similarly and that we may concentrate on only the short-range proton and Λ sources. In this context, we can use Eq. (2) and the pp source function values to extract information about the Λ emission function. We find that $f_\Lambda = \lambda_{\Lambda p}/\sqrt{\lambda_{pp}} = 1.18 \pm 0.40$ and $R_\Lambda = \sqrt{2R^2_{\Lambda p} - R^2_{pp}} = 5.93 \pm 1.30$ fm. Given that $f_\Lambda \simeq 1$, we may argue that all Λ's are made from this source. Such a moderate sized Λ source could indicate the geometrical size of the hot central region of the collision zone, where the energy density is high enough for the production of the strange quarks that form the observed Λ's.

In summary, we have measured small-angle correlations for $p\Lambda$, pp, and $\pi^-\pi^-$ pairs produced in 6A GeV Au + Au reactions and have analyzed them by the source imaging technique [16]. The strong differences in effective source radii reflect very different dynamical histories for each pair. The pp and $\pi^-\pi^-$ pairs may reflect a small homogeneity length caused by flow focusing the source while the Λ emission functions reflect a spread out participant zone.

This work was performed under the auspices of the U.S. Department of Energy by University of California, Lawrence Livermore National Laboratory, under Contract No. W-7405-Eng-48. This work was also supported by NSF Grant No. PHY-00-70818, U.S. DOE Grant No. DE-FG02-88ER40412, and other grants acknowledged in Ref. [19].

[1] H. Stöcker and W. Greiner, Phys. Rep. **137**, 277 (1986).
[2] D. H. Rischke, Nucl. Phys. **A610**, 88c (1996).
[3] H. Sorge, Phys. Rev. Lett. **78**, 2309 (1997).
[4] P. Danielewicz *et al.*, Phys. Rev. Lett. **81**, 2438 (1998).
[5] Quark Matter '96, Proceedings of the 12th International Conference on Ultra-Relativistic Nucleus–Nucleus Collisions, Heidelberg, Germany, 1996, edited by P. Braun-Munzinger *et al.* [Nucl. Phys. A **A610**, 1c (1996)].
[6] C. Pinkenburg *et al.*, Phys. Rev. Lett. **83**, 1295 (1999).
[7] M. Lisa *et al.*, Phys. Rev. Lett. **84**, 2798 (2000).
[8] M. D. Baker *et al.*, Nucl. Phys. **A610**, 213c (1996).
[9] S. Pratt, Nucl. Phys. **A566**, 103c (1993).
[10] H. Boggild *et al.*, Phys. Lett. B **302**, 510 (1993).
[11] H. van Hecke *et al.*, Phys. Rev. Lett. **81**, 5764 (1998).
[12] P. Senger *et al.*, nucl-ex/9810007.
[13] F. Wang and S. Pratt, Phys. Rev. Lett. **83**, 3138 (1999).
[14] L. Ahle *et al.*, Phys. Rev. C **66**, 054906 (2002).
[15] S.V. Akkelin and Y. M. Sinyukov, Z. Phys. C **72**, 501 (1996); U. A. Wiedemann, P. Scotto, and U. Heinz, Phys. Rev. C **53**, 918 (1996); T. Csörgő and B. Löstad, Phys. Rev. C **54**, 1390 (1996).
[16] D. Brown and P. Danielewicz, Phys. Rev. C **64**, 014902 (2001).
[17] S. Y. Panitkin *et al.*, Phys. Rev. Lett. **87**, 112304 (2001).
[18] G. Verde *et al.*, Phys. Rev. C **65**, 054609 (2002).
[19] P. Chung *et al.*, Phys. Rev. Lett. **85**, 940 (2000).
[20] G. Rai *et al.*, IEEE Trans. Nucl. Sci. **37**, 56 (1990).
[21] G. Verde, P. Danielewicz, and D. Brown (to be published).
[22] F. Wang, Phys. Rev. C **60**, 067901 (1999).
[23] S.V. Afanasiev *et al.*, Nucl. Phys. **A698**, 104c (2002).
[24] P.Chung *et al.*, J. Phys. G **28**, 1567 (2002).
[25] S. E. Koonin, Phys. Lett. **70B**, 43 (1977); S. Pratt, T. Csörgö, and T. Zimányi, Phys. Rev. C **42**, 2646 (1990).
[26] W. G. J. Stoks *et al.*, Phys. Rev. C **49**, 2950 (1994).
[27] A. Bodmer and Q. Usmani, Nucl. Phys. **A477**, 621 (1988).
[28] We use this convention so that we can directly compare the Gaussian radii to standard pion radii. This convention is the same as that in Ref. [17].
[29] $R_{1/2} = 1.66 \times R_G$ in Ref. [17]. Assigned uncertainties include the absolute error in data, corrections, and methodology. Hence, they are larger than those in Ref. [17].
[30] S. Panitkin and D. Brown, Phys. Rev. C **61**, 021901 (2000).
[31] The ratio of thermal velocity to expansion velocity for pions will exceed that for protons.
[32] P. Chung *et al.*, Phys. Rev. Lett. **86**, 2533 (2001).